J. Basic. Appl. Sci. Res., 3(2s)639-646, 2013
© 2013, TextRoad Publication

ISSN 2090-4304
Journal of Basic and Applied Scientific Research
www.textroad.com

Coefficient Estimate Flood Flow Channels Comprising Secondary

E. Teymourei[1]*, G.A.Barani[2], H.Janfeshan[3], A. A. Dehghanie[4]

[1] Science and Research branch, Islamic Azad University, Civil Eng Kerman, Sirjan
[2] Co-Professor in Civil Eg, Shahid Bahonar University, Kerman, Kerman
[3] Civil Eng. Faculties of Islamic Azad University, Iran, Golestan, Gorgan
[4] Department of Water Engineering, Gorgan University of Agricultural Sciences and Natural Resources, Golestan, Gorgan

Received: June 10 2013
Accepted: July 10 2013

ABSTRACT

This paper presents a 2D analytical solution for the transverse velocity distribution in compound open channels based on the Shiono and Knight method (SKM), in which the secondary flow coefficient (K-value) is introduced to take into account the effect of the secondary flow. The modeling results agree well with the experimental results from the Science and Engineering Research Council-Flood Channel Facility (SERC-FCF). Based on the SERC-FCF, the effects of geography on the secondary flow coefficient and the reason for such effects are analyzed. The modeling results show that the intensity of the secondary flow is related to the geometry of the section of the compound channel, and the sign of the K-value is related to the rotating direction of the secondary flow cell. This study provides a scientific reference to the selection of the K-value.

KEYWORDS: compound channels, overbank flow, velocity distribution, secondary flow.

1. INTRODUCTION

In alluvial rivers, channels are composed of many different compartments, for example, a main channel with flood plains, in the dry season, the water flow in the main channel, in the rainfalls and flood plains flood water flows flood occurs, then cross the river (flood) occurs. The scientific and practical value for flood relief in the current study there. When the flood flow is studied, hydraulic flow rate is an important parameter. Study of flow behavior in straight channels with flood plains along the channel, the 50 years studied. Of stream channels directly floodplain in 1986 culminated in a flume built Valyngfvrd with 56 meters long and 10 meters wide, which include those on the flume lab worked to be Knight) 1986 (, Celine (1986), Vrmltvn (1986) and cited.

At the time of the flood plain, momentum transfer between main channel and floodplains would be strong. The velocity profile in the main channel and floodplains vary. Therefore it is a suitable method for modeling the velocity distribution is provided. Lateral and depth distributions to predict the average velocity in compound channels, many researchers have proposed various methods. Current analytical models are generally based on the average depth of the model presented by Shyvnv and Knight, is based Of secondary flows due to the impact on the hydraulic flow are important.[5].Despite the low base flows due to the effect of secondary flows on the flow resistance of composite sections in their study is of great importance. The main origin of the difference in shear stress between layers is fluid flows.

Velocity difference between the sections comprising the main channel and flood boundary-layer shear stress in the fluid is produced, which led to formation of secondary flows in this region is [7.20]. Method Shyvnv and Knight analytical solution for the velocity average depth of the equation, N-S provides, that the three parameters of hydraulic coefficient of friction bed flow (f), the coefficient dimensionless viscosity vortex A (λ), the secondary (Γ) there are: Zhou [7] to calculate the flood velocity profiles based on SKM set of formulas that combine the secondary flow and Reynolds stresses are presented, and curve velocity profiles in the main channel and floodplain directly communicate. Erwin and colleagues [4] with the coefficient K for compounds composed of a three-dimensional direct and twisting channels, the secondary flow Γ _d ^ 2 〖〗 KU were replaced, as well as empirical analysis of empirical formula for K obtained . Yang and Gao [8] proposed an analytical Tuesday resolve the eddy viscosity varies based on suitable approximate formulas are obtained by comparison with experimental data. This expression is, that the effect of secondary flow channel consists not only rectangular, but trapezoidal compound channel should not be ignored, and the selection of an appropriate K value will lead to faster and better pressure distribution deals.

2. Introducing the Coefficient of secondary

The momentum equation for the streamwise component of a fluid element can be combined with the continuity equation. Then, we obtain

$$\rho\left[V\frac{\partial u}{\partial y}+w\frac{\partial w}{\partial z}\right]=\rho g\sin\theta+\frac{\partial \tau_{yx}}{\partial y}+\frac{\partial \tau_{zx}}{\partial z} \qquad (1)$$

where U, V, and W are temporal mean velocity components in the x-, y-, and z-directions; τyx and τzx are the Reynolds stresses on planes perpendicular to the y- and z-directions; S0 is the channel bed slope; ρ is the water density; g is the gravitational acceleration.

Shiono and Knight[5] obtained the depth-averaged velocity equation by integrating Eq. (1) over the water depth,

***Corresponding Author:** E. Teymourei, Science and Research branch, Islamic Azad University, Civil Eng Kerman, Sirjan. (Phone: +98-0171-3346-720; fax: +98-0171-3346-720) Teymourei@yahoo.com

$$\rho g H S_0 - \frac{1}{8}\rho f U_d^{\,2}\left(1+\frac{1}{s^2}\right)^{1/2} + \frac{\partial}{\partial y}\left\{\rho\lambda H^2\left(\frac{f}{8}\right)^{1/2} U_d \frac{\partial u_d}{\partial y}\right\} = \frac{\partial}{\partial y}\left[H(\rho UV)_d\right] \qquad (2)$$

P is the density of water, g the acceleration of gravity, H the depth, f Vysbakh Darcy friction factor, U the average velocity depth, s transverse bed slope, y coordinates within the form (1) and λ is the eddy viscosity coefficient is dimensionless. The first term on the left side equation (2) Gravitational attraction, second term, third term conditions, friction and turbulent diffusion. The first term on the right side equation (2) the secondary flow. Kastandv and colleagues [9], respectively; equation combined with (1), based on different assumptions on turbulent diffusion different water depths in the table (1) shown is obtained.

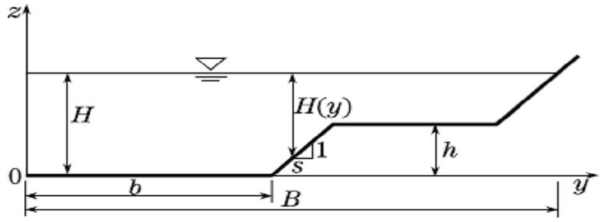

Figure 1. Cross-section of a compound channel with a linear side-slope

Table 1. Three different expressions of the turbulent diffusion term

Model	Expressions of the turbulent diffusion term	Related research
A	$\frac{\partial}{\partial x_j}(\rho H \bar{\varepsilon} A(\frac{\partial U_i}{\partial x_j}+\frac{\partial U_j}{\partial x_i}))$	Ervine et al[5]. ,Shiono and Knight[6] ,Abbott and Price[11], Shome and Steffler[12]
B	$H\frac{\partial}{\partial x_j}(\rho \bar{\varepsilon} A(\frac{\partial U_i}{\partial x_j}+\frac{\partial U_j}{\partial x_i}))$	Stelling et al.[13] ,Blumberg and Mellor[14] ,Roig and King[15], Hu and Kot[16]
C	$\frac{\partial}{\partial x_j}(\rho \bar{\varepsilon} A(\frac{\partial (HU_i)}{\partial x_j}+\frac{\partial (HU_j)}{\partial x_i}))$	Benque et al.[17], Darby and Thorne[18], Balzano[19]

It is not difficult to notice that the three models are equivalent in constant depth areas. However, some studies[9–10] have shown that in the areas of irregular bathymetry with strong depth gradients, Model B can produce the best fit velocity profile compared with the experimental data. Hence, Model B is adopted herein, and then Eq. (2) becomes

$$\rho g H S_0 - \frac{1}{8}\rho f U_d^{\,2}\left(1+\frac{1}{s^2}\right)^{1/2} + H\frac{\partial}{\partial y}\left\{\rho\lambda\left(\frac{f}{8}\right)^{1/2} H U_d \frac{\partial u_d}{\partial y}\right\} = \frac{\partial}{\partial y}\left[H(\rho UV)_d\right] \qquad (3)$$

The difficulty for the solution of the depth-averaged velocity Ud just lies in the determination of the secondary flow term. The traditional method is to divide the cross-section into different panels, and give a constant value Γ for each panel. However, it is apparent that the secondary flow term H(ρUV)d has a close relation with the velocity distribution. Therefore, the assumption proposed by Ervine et al.[4] is adopted, which associates the secondary flow term with the depth-averaged velocity shown in

$$UV = kU_d^2 \qquad (4)$$

Substitute Eq. (4) into Eq. (3). Then, the partial differential equation (3) can be transformed into the ordinary differential equation,

$$\rho g H S_0 - \frac{1}{8}\rho f U_d^{\,2}\left(1+\frac{1}{s^2}\right)^{1/2} + H\frac{\partial}{\partial y}\left\{\rho\lambda\left(\frac{f}{8}\right)^{1/2} H U_d \frac{\partial U_d}{\partial y} - \rho K U_d^2\right\} - \frac{\partial H}{\partial y}\rho K U_d^2 = 0 \qquad (5)$$

Equation (5) is a second-order constant coefficient linear ordinary differential inhomogeneous equation, whose solution is equal to a special solution plus the general solution of the corresponding homogeneous equation. The analytical solution of Eq. (5) is given as follows:

1- For constant depth areas in the main channel and on the floodplain, there exists

$$U_d = \sqrt{\frac{8}{\rho f}\left[\beta + C_1 \exp(\frac{-2}{e+\sqrt{4a+e^2}}y) + C_2 \exp(\frac{-2}{e-\sqrt{4a+e^2}}y)\right]} \qquad (6)$$

Where $a = \frac{\lambda H^2}{2}(\frac{8}{f})^{1/2}, \beta = \rho g H S_\circ, e = \frac{8KH}{f}$, and C_1 and C_2 are unknown constants.

2- For the linear side slope domain shown in Fig. 1, the depth function is given by

$$H(y) = H - \frac{y-b}{s} \qquad (7)$$

where s is the side slope of the main channel, and the other variables are illustrated in Fig. 1. Substituting Eq. (7) into Eq. (5), we can obtain the analytical solution of the depth-averaged velocity in the linear side slope domain,

$$U_d = \sqrt{\frac{8}{\rho f}\left(\frac{P}{M+N}H(y) + C_1 H(y)\frac{L+M-\sqrt{(L+M)^2+4LN}}{2L} + C_2 H(y)\frac{L+M+\sqrt{(L+M)^2+4LN}}{2L}\right)} \quad (8)$$

Where $P = \rho g S_\circ, L = \frac{\lambda}{S^2}\left(\frac{2}{f}\right)^{1/2}, M = -L - \frac{8K}{fs}, N = \left(1+\frac{1}{S^2}\right)^{1/2} - \frac{8K}{fs}$, and C_1 and C_2 are unknown constants.

3. Boundary conditions

In the modeling, the cross-section is generally divided into several panels, as shown in Fig. 2. Through the above analysis, C1 and C2 can be solved, provided that the appropriate boundary conditions are specified. One boundary condition is the no-slip boundary condition, that is, U=0 at the remote boundaries; the other is the requirement for continuity at the interface between domains. The boundary conditions are as follows:

1-For symmetry, the velocity gradient in the centerline of the main channel must be zero,

$$\left.\frac{\partial U_d}{\partial y}\right|_{y=0} = 0$$

2-At the panel interface, the continuity of the velocity and the velocity gradient should be satisfied, i.e.,

$$U_i = U_{i+1} \text{ and } \frac{\partial U_i}{\partial y} = \frac{\partial U_{i+1}}{\partial y}$$

3- The velocity must be zero at the edge of the floodplain.

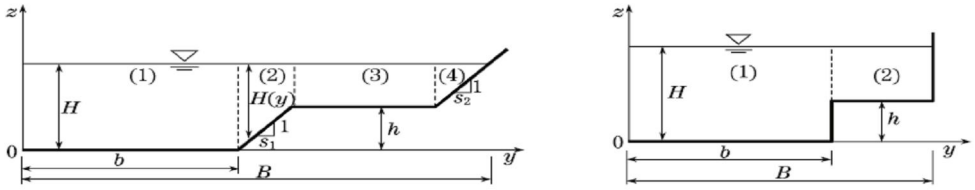

(a) Trapezoidal Compound channels (b) Rectangular Compound channels

Figure 2. Geometries of compound channels

4. Determination of the parameters

From the above analysis, it is not difficult to know that the depth-averaged velocity distribution can be obtained if the parameters in each panel were determined: the dimensionless eddy viscosity(λ), the Darcy-Weisbach friction factor(f), and the secondary flow coefficient (k). Shiono and Knight[5] have shown that the velocity profile is insensitive to the dimensionless eddy viscosity λ, and even a standard value λ= 0.07 in the whole cross-section can give satisfactory results. To simplify the calibration procedure, and to make the modeling work easier, a constant "standard" value of λ for all the models (λ= 0.07) is assumed herein. The Darcy-Weisbach friction factors for the main channel and the floodplain can be determined based on the zonal bed shear stress,

$$f = \frac{8\tau_b}{\rho U_d^2} \quad (9)$$

Hence, only the secondary current term(K) requires calibration in order to model the velocity distribution. Ervine[4] presented the empirical formula for K through the analysis of a great deal of experimental data. For straight compound channels, K < 0.5%; for meandering compound channels, K is related to the sinuosity of rivers, relative depth, and relative roughness. However, there is no robust relationship.

The present researches on the secondary flow coefficient are few, and the adoption of the value

is empirical[4-6,16–19]. In addition, it is generally considered that the K-value in the main channel is a constant, while zero on the floodplain, whether in straight compound channels or meandering compound channels. Ervine[4] indicated that the K-value must be specified differently in the main channel and on the floodplain. However, he assumed the K-value on the floodplain to be zero in actual simulations, which did not coincide with the structure of the secondary flow in compound channels. Literature [17] pointed out that the secondary flow cells in compound channels (straight and meandering compound channels) are complex and the delicate division of the compound channel section would be necessary if we want to produce the precise distribution of the velocity and the shear stress. A similar suggestion can be seen in the literatures [4–6, 9, 14–19], which also emphasize the importance of the secondary flow cells in the modeling.

In the present paper, the SERC-FCF experimental data series are used to verify and analyze the modeling results. The previous research based on the SERC-FCF experimental data indicated the complexity of the secondary flow cells in straight compound channels. Thus, ignorance of it would produce inaccuracy[4–6,9,16–19]. To study the variation law of the secondary flow coefficient, the compound channel is divided into different subsections (main channel subsection, floodplain subsection, and conjunction subsection, as shown in Fig. 1). The respective K-value in each panel is determined through the best fit procedure, based on which the influence of the geometries to the secondary flow coefficient is analyzed.

4. Influence of the geometries to the K-value

Experimental setup In the SERC-FCF experimental data series, Series 01, 02, and 03 covered different floodplain widths with the main channel side slope s1 of 1:1 (horizontal length:vertical length). Series 02, 08, and 10 kept the floodplain widths constant, but covered main channel side slopes of 1:1, :1,2:1. Series 02 and 07 provided a comparison between smooth floodplains and rough floodplains. The geometries of symmetrical compound channels are shown in Fig. 1, and the geometry details of the series mentioned above are shown in Table 2.

Table 2. Geometry details of the symmetric compound channels for eleven series

Series No.	*b*/m	*h*/m	H/m	*B*/*b*	*s*1	Floodplain type
FCF0106	1	6.67	0.215	0.15	0.75	Smooth
FCF0203	1	4.20	0.177	0.15	0.75	Smooth
FCF0205	1	4.20	0200	0.15	0.75	Smooth
FCF0206	1	4.20	0.215	0.15	0.75	Smooth
FCF0302	1	2.40	0.166	0.15	0.75	Smooth
FCF0305	1	2.40	0.200	0.15	0.75	Smooth
FCF0306	1	2.40	0.215	0.15	0.75	Smooth
FCF0308	1	2.40	0.300	0.15	0.75	Smooth
FCF0703	1	4.20	0.177	0.15	0.75	Rough
FCF0805	0	4.00	0.200	0.15	0.75	Smooth
FCF1005	2	4.40	0.200	0.15	0.75	Smooth

5. Influence of the depth on the floodplain

Three tests (Series 0302, 0305, and 0308) are adopted to examine the effect of the water depth on the floodplain, which are 0.166 m, 0.200 m, and 0.300 m, respectively. These are all with the same actual floodplain width as well as the same main channel side slope. Figure 3 shows that with the increase of the depth on the floodplain, the absolute values of K in the three domains are gradually decreasing (the comparison of the K-value is just the comparison of the absolute value of K in the following parts). This is because when the depth on the floodplain is larger, the velocity distribution in the whole cross-section will be more homogeneous, and the transverse velocity V is relatively small compared with the streamwise velocity U. Thus, a smaller secondary flow coefficient would not be surprising, which will be mentioned in Section 5.

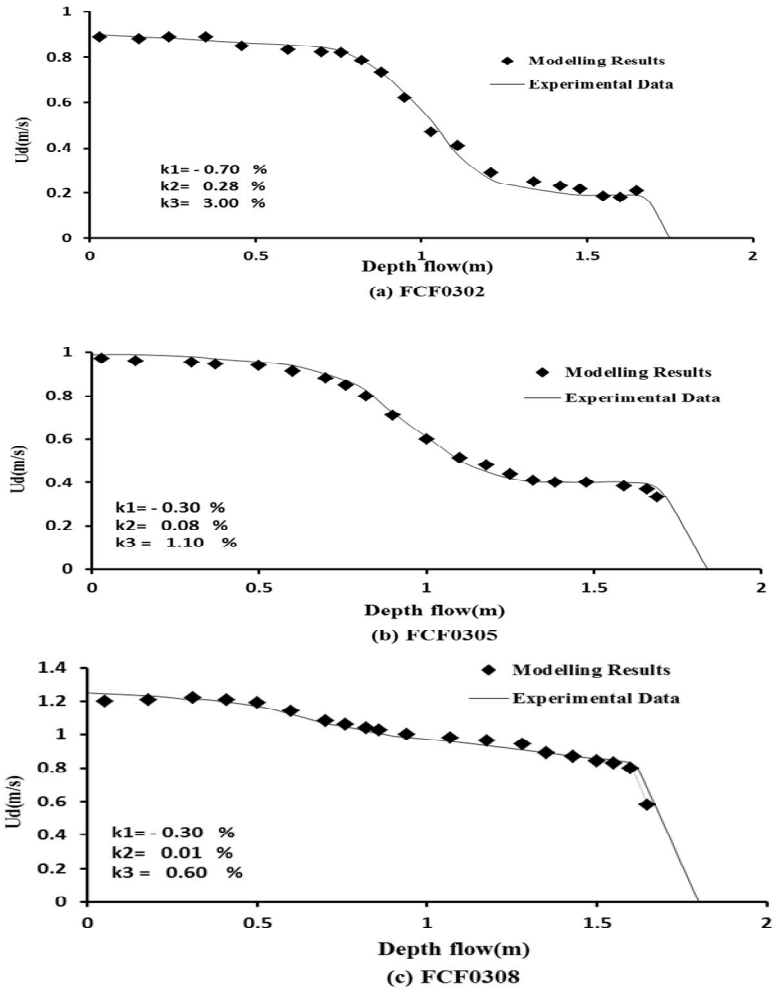

Figure 3. Influence of the depth on the floodplain

6. Influence of the width on the floodplain

A total of three tests (Series 0106, 0206, and 0306) were used to examine the influence of the floodplain width, which are 4.1 m, 2.25 m, and 0.75 m, respectively. These are all with the same actual floodplain water depth as well as the same main channel side slope.

It can be illustrated from Fig. 4 that with the decrease of the floodplain width, the K-value on the floodplain increases, while the K-values in the main channel and side slope domain decrease gradually. This is because when the floodplain width is smaller, the 3D mixing process will be more obvious, and the effect of the secondary flow becomes more intense.

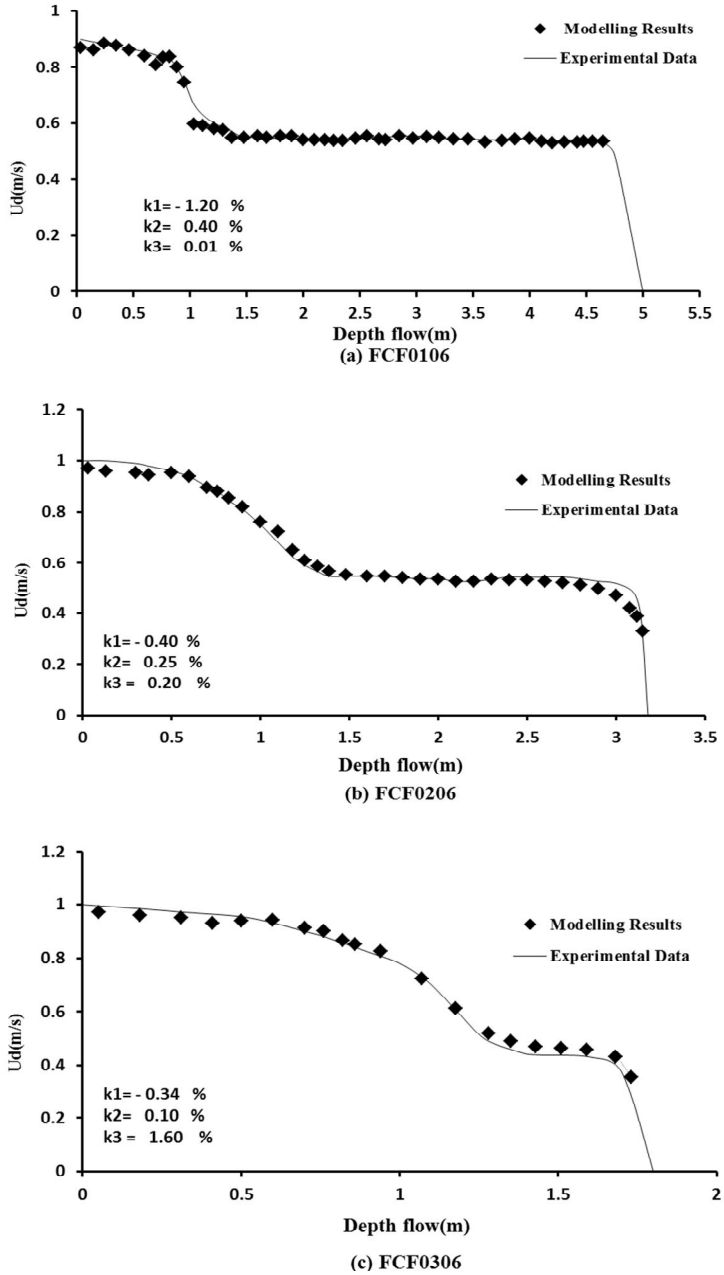

Figure 4. Influence of the width of the floodplain

7. Influence of the main channel side slope

Three tests (Series 0805, 0205, and 1005) are taken to examine the influence of the main channel side slope, with s being 0:1, 1:1, 2:1, respectively, yet with the same floodplain width as well as the same water depth on the floodplain. Figure 5 indicates that with the increase of the main channel side slope, the K-value in the main channel increases, while the K-values on the floodplain have the relation KFCF1005 > KFCF0805 >KFCF0205, and the K-value in the side slope domain is decreasing. The reason is that with a smaller side slope, the effect of the secondary flow becomes more intense, while the influence scope weakens gradually, which is responsible for the erosion of the river bed and banks. Also, go against the stability of the riverbed and the propagation of animals and plants, then destroy the ecosystem of the river.

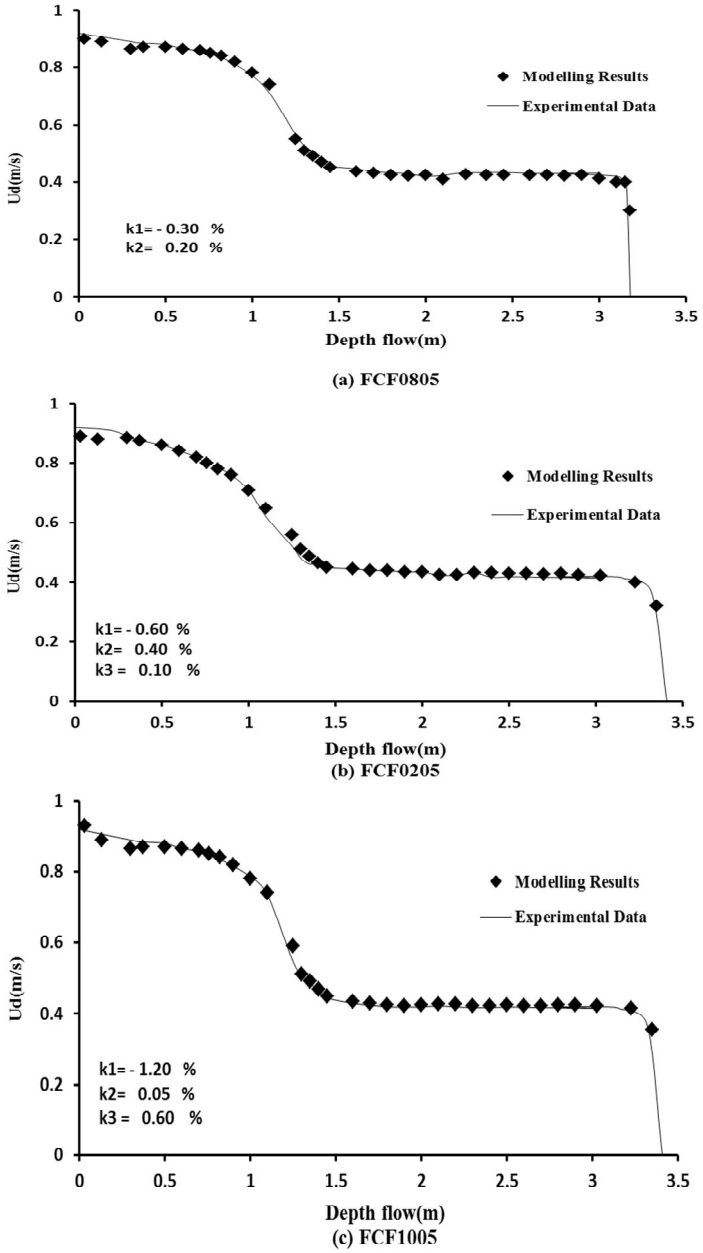

Figure 5. Influence of the main channel side slope

8. Influence of the roughness on the floodplain

Two tests (Series 0203 and 0703) are available to examine the influence of the floodplain roughness, in which Series 0203 is for the smooth floodplain and 0703 for the rough floodplain, but with the same water depth on the floodplain and the same main channel side slope. Fig ure 6 illustrates that when the floodplain is rough, the K-values in the three domainsare gradually increasing. This is expected because as the roughness of the floodplain becomes larger, the velocity on the floodplain decreases while it increases in the main channel, causing more velocity difference between the main channel and the floodplain. It is inevitable that the momentum transfer becomes stronger when the velocity difference is larger. Thus, the secondary flow coefficients become larger in the whole cross-section.

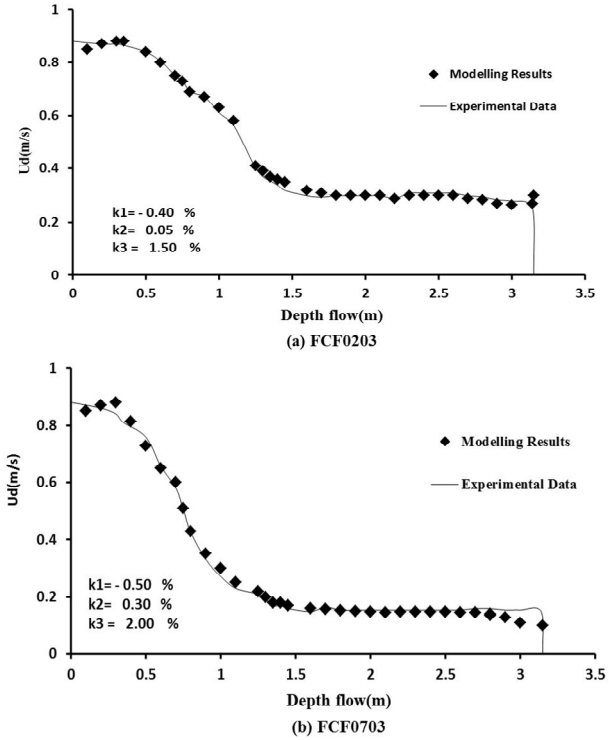

Figure 6. Influence of the roughness of the floodplain

9. Analysis of the secondary flow coefficient

From the original definition of the K-value in the literature [4], it was used to represent the relation of $(UV)_d$ and U_d^2 , which assumed that the temporal mean velocity components (U, V) are fractions of the depth-averaged velocity. Ikeda[16] developed an analytical expression for the transverse velocity V , as

$$\frac{V}{U_*} = \frac{6\delta}{k\pi^2} Sin(\frac{\pi y}{H})\left[2Cos(\frac{\pi z}{H}) - \pi(\frac{2z}{H} - 1)Sin(\frac{\pi z}{H}) \right] \quad (9)$$

where U_* is the shear velocity,k is von Karman's constant (k=0.415), and δ is the dimensional amplitude of perturbation. Then, the transverse velocity V could be either positive or negative due to Eq. (9), and we can obtain that the depth-averaged product of $UV, (UV)_d$,could be either positive or negative. From the analysis in Subsections 5.1–5.5, the K-value is always negative in the main channel while positive on the floodplain, and even larger than %0.5 in some cases, which indicates that the proposal of Ervine et al. assuming that K is positive is not always appropriate. The value of $(UV)_d$ could be positive for clockwise current cells (along the streamwise direction) and negative for anti-clockwise current cells, as shown by Chlebek and Knight[19] and Knight et al.[14], which is also in accordance with the present paper.

10. Conclusions

The present paper analyzed the variation law of the secondary flow coefficient with the geometries based on the best fit procedure with the SERC-FCF experimental data. The following conclusions can be drawn.

(i) With the increase of the depth on the floodplain, the velocity distribution in the whole cross-section becomes more homogeneous, and the secondary flow coefficients in the three domains tend to decrease gradually.

(ii) With the decrease of the floodplain width, the K-value on the floodplain increases, while the K-values in the main channel and the side slope domain are gradually decreasing.

(iii) With the increase of the main channel side slope, the K-value in the main channel increases, while the K-value on the floodplain is not so, with the rectangular compound channel in the middle, and for trapezoid compound channels, the K-value on the floodplain increases with the side slope, while the K-value in the side slope domain varies contrarily, that is, decreases with the side slope.

(iv) When the floodplain is rough, the velocity difference between the main channel and the floodplain becomes larger. Thus, the momentum transfer becomes stronger and the secondary flow coefficients become larger in the whole cross-section.

The above conclusions indicate that the determination of the K-value in each domain is crucial for modeling the velocity distribution in compound open channels, and the variation law of the secondary flow coefficient is directly related with the structure of the secondary flow. The results of the present paper propose a preliminary reference for the selection of the Kvalue. However, it may need more experimental verification and further research. Furthermore, for compound

channels with complex geography, such as meandering compound channels and compound channels with vegetated floodplain, the structure of the secondary flow and the effect of vegetation on the secondary flow structure will be more complex, and more attention should be further given.

REFERENCES

1. Yang, K., Cao, S., and Knight, D. W.:Flow patterns in compound channels with vegetated floodplains. Journal of Hydraulic Engineering 133(2), 2007, 148–159
2. Zhang, M., Shen, Y., andWu, X: 3D numerical simulation on overbank flows in compound channels (in Chinese). Journal of Hydroelectric Engineering 25(5), 2006. 31–36
3. Huai, W., Chen, W., and Tong, H. :3D numerical simulation on overbank steady open channel flows in compound channels (in Chinese). Advances in Water Science 14(1), 2003. 15–19
4. Ervine, D. A., Babaeyan-Koopaei, K., and Sellin, R. H. J. Two-dimensional solution for straight and meandering overbank flows. Journal of Hydraulic Engineering 126(9), 2000, 653–669
5. Huai, W., Xu, Z., Yang, Z., and Zeng, Y.Two dimensional analytical solution for a partially vegetated compound channel flow. Applied Mathematics and Mechanics (English Edition) 29(8), 2008.1077–1084 DOI 10.1007/s10483-008-0811-y
6. Xu, W. :Study on computational method of overbank flow in channels with compound cross section (in Chinese). Journal of Hydraulic Engineering (6), 2001, 21–26
7. Yang, Z. H. and Gao, W. :Two dimensional analytical solution for overbank flows with interaction between the main channel and floodplain (in Chinese). Journal of Sichuan University (Engineering Science Edition) 41(5), 2001, 42–46
8. Castanedo, S., Medina, R., and Mendez, F. J. :Models for the turbulent diffusion terms of shallow water equations. Journal of Hydraulic Engineering 131(3), 2005, 217–223
9. Abbott, M. B. and Price, W. A. Coastal, :Estuarial, and Harbour Engineers' Reference Book, 1994,Taylor & Francis, London/New York
10. Shome, M. L. and Steffler, P. M.Lateral flow exchange in transient compound channel flow.Journal of Hydraulic Engineering 124(1), 1998, 77–80
11. Stelling, G. S., Wiersma, A. K., and Willemse, J:Practical aspects of accurate tidal computations. Journal of Hydraulic Engineering 112(9), 1986, 802–817
12. Blumberg, A. F. and Mellor, G. L. A description of a three-dimensional coastal ocean circulation model. Three-Dimensional Coastal Ocean Models (ed. Heaps, N. S.), American Geophysical Union, Washington, DC, 1987, 1–16
13. Huai, W., Gao, M., Zeng, Y., and Li, D. Two-dimensional analytical solution for compound channel flows with vegetated floodplains. Applied Mathematics and Mechanics (English Edition) 30(9), 2009, 1121–1130 DOI 10.1007/s10483-009-0906-z
14. Tang, X. and Knight, D. W. A general model of lateral depth-averaged velocity distributions for open channel flows. Advances in Water Resources 31(5), 2008, 846–857
15. Knight, D. W., Omran, M., and Tang, X. Modeling depth-averaged velocity and boundary shear in trapezoidal channels with secondary flows. Journal of Hydraulic Engineering133(1), 2007,39–47
16. McGahey, C. A Practical Approach to Estimating the Flow Capacity of Rivers Application and Analysis, Ph. D. dissertation, Open University, Milton Keynes, UK , 2006
17. Ikeda, S.Self-formed straight channels in sandy beds. Journal of the Hydraulics Division 107(4), 1981,389–406
18. Chlebek, J. and Knight, D. W. A new perspective on sidewall correction procedures, based on SKM modelling. Proceedings of the International Conference on Fluvial Hydraulics (eds. Ferreira, R. M. L., Alves, E. C. T. L., Leal, J. G. A. B., and Cardosa, A. H.), Taylor & Francis, London/NewYork, 2006,135–144
19. Byjad. K., M. Small. Salah, Mohammad Ayub. SA,:The effect of slope on secondary currents in compound levels using a two-dimensional model of momentum over, 2012,Iranian Journal of Soil and Water Research, Volume 41, Number2.